IEEE Access
Multidisciplinary | Rapid Review | Open Access Journal

SPECIAL SECTION ON EMERGING TECHNOLOGIES ON VEHICLE TO EVERYTHING (V2X)

Received December 15, 2018, accepted January 6, 2019, date of publication January 14, 2019, date of current version February 6, 2019.

Digital Object Identifier 10.1109/ACCESS.2019.2892979

A Relay-Node Selection on Curve Road in Vehicular Networks

DUN CAO[1,2], (Member, IEEE), YONGHE LIU[3], XIAOMIN MA[4], (Senior Member, IEEE), JIN WANG[1], (Senior Member, IEEE), BAOFENG JI[5], CHUNHAI FENG[3], AND JINXIU SI[6]

[1]School of Computer and Communications Engineering, Changsha University of Science and Technology, Changsha 410114, China
[2]Hunan Provincial Key Laboratory of Intelligent Processing of Big Data on Transportation, Changsha 410114, China
[3]Department of Computer Science and Engineering, The University of Texas at Arlington, Arlington, TX 76019, USA
[4]College of Science and Engineering, Oral Roberts University, Tulsa, OK 74171, USA
[5]College of Information Engineering, Henan University of Science and Technology, Luoyang 471000, China
[6]School of Information and Communication Engineering, University of Electronic Science and Technology of China, Chengdu 611731, China

Corresponding author: Jin Wang (jinwang@csust.edu.cn)

This work was supported in part by the National Natural Science Foundation of China under Grant 51675059, Grant 61702052, Grant 61801170, Grant 61501405, Grant 61671144, and Grant 61772087, in part by the National 13th Five National Defense Fund under Grant 6140311030207, and in part by the Scientific Research Fund of Hunan Provincial Education Department under Grant 17B011.

ABSTRACT In vehicular networks, the selection of the relay-node determines the message dissemination through the vehicle-to-vehicle communication. However, the irregular shape of the curve road makes it difficult to design and analyze the relay-node selection on the curve road. In this paper, a relay-node selection on the curve road is first proposed, which aims to fast message delivery and complete coverage of the curve road, namely the complete relay-node selection. Additionally, after defining a metric of the curving rate, the models are constructed to analyze the performances of our proposal in terms of the message dissemination speed and the packet delivery rate. Simulations on a realistic mountain road are conducted. Moreover, the up-to-date relay-node selection methods are adapted to suit the scenario of the curve road for the comparison. The results of the simulations prove the validation of the analytic models and the significant performances of our proposal. The attractive benefits include not only the stable performance against the vehicle density in terms of the message dissemination speed and the packet delivery rate but also the improvements of at least 16.20% gain compared with these adapted methods in terms of the message dissemination speed as well as the packet delivery rate of more than 99.7%.

INDEX TERMS Relay-node selection, curve road, vehicle-to-vehicle communication, vehicular networks.

I. INTRODUCTION

On the mountain road, the limited vision for drivers due to full of sharp turns causes the frequent occurrence of traffic accidents. The same event also happens on the ramp of the highway. The safety application in vehicular networks is expected to be an effective method to avoid the problem. In vehicular networks, the critical message is shared between the nodes (e.g., vehicle, infrastructure, and pedestrian) through the communication technologies of Vehicle to Everything (V2X) [1]–[4]. In these technologies, Vehicle-to-Vehicle (V2V) plays an important role with the advantage of the direct discovery, flexible structure and economic efficiency. The utilization of the relay-nodes among vehicles can extend the coverage of messages. And the relay node selection determines the efficiency and reliability of the message dissemination in vehicular networks.

In the relay-node selection methods, the geography-based method outperforms other methods since it is benefited from the prior knowledge of the local road structure [5], [6]. However, the existing works focus on the scenarios of the intersection and the straight road, and few contributes to the relay-node selection on the curve road.

Bi *et al.* [7] and Suthaputchakun *et al.* [8] respectively proposed the Position-based Multi-hop Broadcast Protocol (PMBP) and the Trinary Partitioned Black-Burst-based Broadcast protocol (3P3B) to select the relay-node on the straight road. Whereas, in [9], Korkmaz *et al.* developed the Urban Multi-hop Broadcast protocol (UMB) and Ad hoc Multihop Broadcast (AMB), which can be applied on the intersection. Additionally, Sahoo *et al.* explored the Binary-Partition-Assisted Broadcast protocol (BPAB) in [10], which can be applied on both the straight road and the intersection.

Moreover, in our earlier works [11]–[13], we developed an exponential partition mechanism and designed two methods which are suitable to the scenarios of the above two road structures, respectively. It is known that the curve road is another typical road structure. And the vehicular network on the curve road is 2-dimension (2-D) network like the network on the intersection. However, the curve road does not have the describable shape like the intersection, and this makes it difficult to select the relay-node according to the shape of the curve road. In the known Greedy Perimeter Stateless Routing (GPSR) [14], Karp and Kung designed a greedy forwarding decisions in 2-D mobile ad hoc network. However, the information of the road structure is hoped to be used for the performance improvement of the relay-node selection on the curve road.

A few works discussed the relay-node selection on the curve road. In [15], Wu *et al.* defined the intended area where the message is expected to be delivered in some special scenarios like the curve road to cover the curve road completely. Naumov and Gross [16] and Bernsen and Manivannan [17] selected the node on the road curve as the anchor point to deliver the message. However, the procedure of the relay-node selection on the curve road was not discussed in these works.

Valuable works have been done in the modeling and analysis of the relay-node selection [8], [10]–[13], [18]–[23]. And the performance expression can validate and optimize these method. In these works, [8] and [10] analyzed the performances of the methods in these literature on the straight road in terms of the message transmission speed. We also built the performance model for our exponential-partition-based relay-node selection on the straight road and the general intersection in terms of the message transmission speed and Package Delivery Rate (PDR) in [11]–[13]. Moreover, some performance analyses have been conducted on the methods in the 2-dimension vehicular network in [20] and [21], without including the influence of the road structure. More efforts are needed to obtain the closed-form expression for the performance of these geography-based method on the curve road.

In this paper, to the best of our knowledge, a relay-node selection method on the curve road is first proposed, namely the complete relay-node selection method. The contributions are threefold: 1) through defining the optimal position and the partition range, a general exponent-based partition method is improved on the curve road to obtain a stable performance; 2) after designing the double-direction relay-node selection, a complete relay-node selection method is developed to assure the message cover all area on the curve road; 3) A metric of the curving rate is defined to measure the bending degree of the curve road, and the performances of our proposal are analyzed in terms of the message dissemination speed and PDR for the validation and the further optimization of our proposal.

The remainder of this paper is organized as follows. In Section II, a strategy for the relay-node selection on the curve road is developed. In Section III and Section IV, a general exponent-based partition method and a complete relay-node selection method on the curve road are explored, respectively. Additionally, after the definition of a metric of the curving rate, the models for the performances of our proposal in terms of the message dissemination speed and PDR are developed in Section V. Section VI presents the simulations on a realistic mountain road to validate these models and to evaluate our proposal. To verify the improvement of our proposal, the mentioned methods based on the geographical information are adapted to fit the curve road for comparison. Finally, our work is summarized in Section VII.

II. STRATEGY OF THE RELAY-NODE SELECTION ON CURVE ROAD

Aiming to deliver the message as fast as possible, the relay-node selection method on the curve road searches the furthest node from the sender in one hop along the road. Following the guideline, we define an *optimal position* $\mathrm{P_{opt}}$, at which the relay-node can cover the maximum distance from the sender and achieve the message progress of 100%. As shown in Figure 1, the $\mathrm{P_{opt}}$ for the sender is located at the farthest one among the junctions of the communication range R_{sender} of the sender and the curve road, marked with the symbol of "+". In this paper, assume that every node has the same communication range R and is equipped with the positioning system and Geographic Information System (GIS) service to get the information of own location and the local road. The mechanism of Request-To-Broadcast/Clear-To-Broadcast (RTB/CTB) is adopted to indicate the start and the end of the relay-node selection and meanwhile to avoid the hidden node problem in vehicular networks. Moreover, in our proposal, only one node is chose as the relay-node to prevent the broadcast storm. The basic mechanism of the relay-node selection on the curve road is described as follows:

- The sender accesses the channel and broadcasts a RTB package. The package in our proposal includes the locations of the sender.
- The nodes receiving the RTB in the message dissemination direction deduce that they are in the communication range of the sender. And then these nodes compute the $\mathrm{P_{opt}}$ with the sender's location and the GIS. Since the relay-node is at least nearer to $\mathrm{P_{opt}}$ than the sender, the nodes participating in the relay-node selection should also be in the circular range $R_{\mathrm{P_{opt}}}$ of radius R centered at $\mathrm{P_{opt}}$. In the example of Figure 1, these candidate nodes are marked with the black solid circle "•". It is worthy to note from Figure 1 that there are several junctions of R_{sender} and the road, and some nodes on the road section from the sender to $\mathrm{P_{opt}}$ do not lie in R_{sender}. Besides, the nodes that are in R_{sender} but out of $R_{\mathrm{P_{opt}}}$ maybe exist, for example the node in Figure 1 marked with the gray solid circle between $\mathrm{P_A}$ and $\mathrm{P_B}$.
- Among these candidate nodes, the nearest node to $\mathrm{P_{opt}}$ is selected as the relay-node. Then the relay-node sends a CTB package to the sender, and the handshake between the sender and the relay-node is completed.

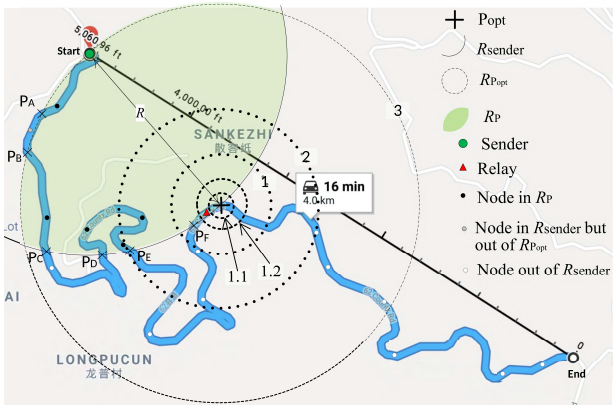

FIGURE 1. Strategy of the relay selection on the curve road.

The selection of the nearest node is processed with the general exponent-based partition method originated from our earlier work [11]. The general exponent-based partition method will be developed in the next section.

- The relay-node broadcasts the message to the nodes in its communication range. The receiving of the same message at the sender is a successful confirmation of the relay-node selection. From the whole procedure, it can be seen that the nodes in the merged range of R_{sender} and $R_{\text{relay-node}}$ can receive the message. $R_{\text{relay-node}}$ represents the communication range of the relay-node.

In this section and the following section, for simplicity yet effective application, the Euclidean Distance is adopted to judge the geographic distance.

Define the common area of the circles centered at the sender and the P_{opt} as the *partition range* R_{p}. In the example of Figure 1, the nodes in the R_{p} can enter the partition phase. However, in the real world, the Non-Line of Sight (NLOS) because of the tall trees and the mountain body may lead to only part of the nodes in the R_{p} receive the RTB package and work as the candidate nodes. Thus, in realistic scenarios the relay-node is selected among the nodes that have qualified communication channels from the sender in one-hop.

For clear exposition, the primary notations throughout this paper are summarized in Table 1.

III. GENERAL EXPONENT-BASED PARTITION ON CURVE ROAD

The candidate nodes in the partition range R_{p} get involved in the selection of the relay-node. A general exponent-based partition (GEP) is employed to pick up the relay-node from these candidate nodes on the curve road. GEP is improved from our earlier work which is adopted on the straight road with the help of the black burst (B). The detail of GEP is shown in Figure 2 and described as follows.

- According to the distance to P_{opt}, R_{P} (the area from the starting position to the optimal position shown in Figure 2) is divided into N_{part} segments with N_{iter} iterations. The width of the k-th segment in the j-th iteration

TABLE 1. Summary of notations.

Notations	Descriptions
P_{opt}	Optimal position
R_{C}	Circular range of radius R centered at C
R	Communication range
R_{p}	Partition range
B	Black burst
N_{part}	Number of partition in each iteration
N_{iter}	Number of iteration
k	Index of the k-th segment
j	Index of the j-th iteration
$W_{\text{seg}}(j,k)$	Width of the k-th segment in the j-th iteration
A	Compression coefficient
i	Index of the i-th segment in the j-th iteration
$C_{\text{w}}(c)$	Maximal number of back-off timers in the c-th contention
c	Index of the c-th CTB-contention
γ	Curving rate
$L_{C,D}$	Length of the road between C and D
β	Message progress
$L_{\max}$	Maximum message dissemination distance
$v_{\max}$	Maximum speed of vehicles
T_{d}	One-hop delay
T_{init}	Initial latency
T_{part}	Average partition latency
T_{cont}	Average contention latency
T_{data}	Data transmission latency
PDR	Package delivery Rate
n	Number of vehicles
λ	Vehicle density
$\mu_{\text{p\_range}}$	Average vehicle numbers in the partition range
$\mu_{\text{seg}}^{j,k}$	Average vehicle numbers in the k-th segment of the j-th iteration
$\gamma_{\text{seg}}^{j,k}$	Curving rate in the k-th segment of the j-th iteration
$P_{\text{seg\_sel}}^{j,k}$	Probability of the selection of the k-th segment in the j-th iteration
$\mu_{\text{seg\_bro}}^{j,i}$	Average vehicle numbers in other segments in the message dissemination direction when the i-th segment is selected in the j-th iteration
$N_{\text{P\_slot}}(k)$	Number of time-slots spent when the k-th segment is selected
$p_{\text{suc\_con}}^{k,c}$	Single probability of the success case in the c-th contention of the k-th final segment
$p_{\text{col\_con}}^{k,c}$	Single probability of the collision case in the c-th contention of the k-th final segment
μ_k	Average vehicle numbers in the k-th segment of the N_{iter}-th iteration
p_c	Probability of the selection of a back-off timers in the c-th contention
$p_{\text{suc}}^{k,c}$	Whole success probability after c contentions in the k-th final segment
$T_{\text{con\_seg}}^{k}$	Contention latency of the k-th segment
$T_{\text{col}}(c)$	Duration spent in the collision case in the c-th contention
$T_{\text{suc}}(c)$	Duration spent in the success case in the c-th contention
$P_{\text{seg\_sel}}^{k}$	Probability of the selection of the k-th segment in the N_{iter}-th iteration
M_k	Average message progress for the k-th final segment
N_{recon}	Number of the contention re-attempt
$p_{\text{fail\_seg}}^{k}$	Probability of the selection failure in the k-th final segment
$p_{\text{fail\_seg}}$	Probability of the selection failure in one-hop
$v_{\text{max\_rule}}$	Limit speed in a specific road scenario
$v_{\max}$	Maximum speed of the vehicle
$d_{\text{inter\_veh}}$	Average inter-vehicle distance

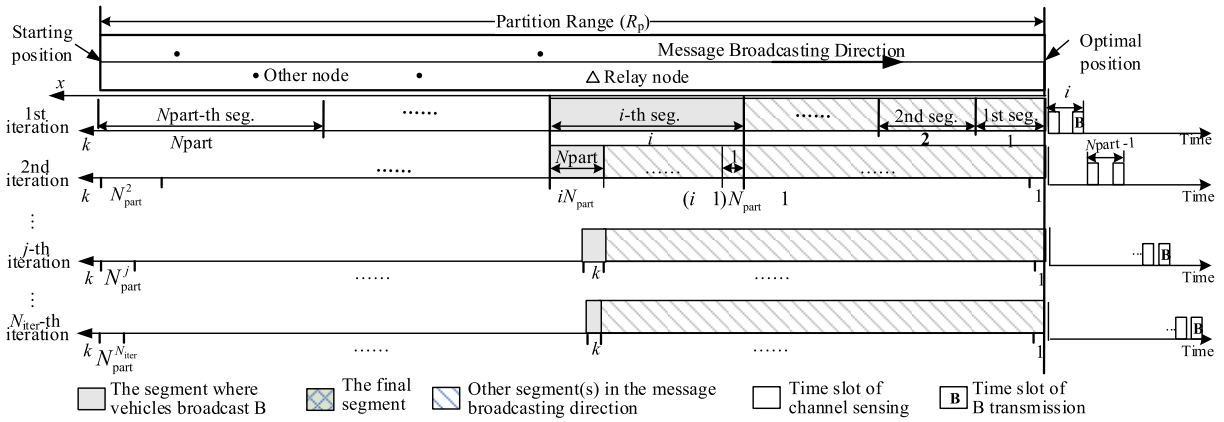

FIGURE 2. Procedure of the general exponent-based partition.

can be computed as

$$W_{\text{seg}}(j,k) = \frac{1}{A}\left[(1+A)^{\frac{((k-1) \bmod N_{\text{part}})+1}{N_{\text{part}}}} - (1+A)^{\frac{(k-1) \bmod N_{\text{part}}}{N_{\text{part}}}}\right] W_{\text{seg}}\left(j-1, \left\lceil \frac{k}{N_{\text{part}}} \right\rceil\right), \quad (1)$$

where A is a compression coefficient. And the bigger is A, the thinner is the segment closest to the P_{opt}. $\lceil \bullet \rceil$ presents the ceiling function. The derivation of the above equation can be seen in [12]. After receiving the RTB packet, all nodes in R_p determine the segment they locate in, and broadcast a B in the corresponding time-slot. The nodes in the segment closer to the P_{opt} broadcast the B earlier;

- If sensing a B before sending its B, the node quits the relay selection procedure. Since the node deduces that there are nodes closer to the P_{opt} than itself;
- The nodes, having broadcast the B, get into the next iteration. The partition procedure is repeated for N_{iter} times, and the final segment, which is nonempty and closest to the optimal position, is selected;
- The nodes in the final segment contend for the relay node by randomly selecting a back-off timer to avoid collision. Finally, the node, the back-off times of which ends first, wins as the relay node. To save the time, when the selected segment in an iteration is the N_{part}-th segment, the nodes in the final segment enter next iteration without sending the B.

In the 1st iteration of the example in Figure 2, the node in the i-th segment broadcasts a B in the i-th time-slot, then other nodes sense the B and quit the partition. The node in the i-th segment joins in the 2nd iteration. In the and iteration, the node only exists in the N_{part} segment, thus the node directly continues the 3rd iteration without sending the B. The similar process continues for N_{iter} iterations totally. Finally, the node in k-th segment of the N_{iter} -th iteration enters the CTB-contention to be selected as the relay-node.

Figure 1 illustrates the procedure of GEP on the curve road. $(N_{\text{iter}}, N_{\text{part}}, A) = (2, 3, 2.3)$ in the example. The nodes that receive the RTB package, i.e., the candidate nodes, calculate the distance between themselves and the P_{opt}, respectively. If the node finds its distance is larger than R, it quits the relay-node selection. Thus, only these nodes marked with the black solid circle enter the partition. According to the distance, the partition range in the first iteration is split into three segments by the circles labeled with 1, 2, and 3. In the direction from the P_{opt} to the sender, the segments are referred as the 1st segment, the 2nd segment, and the 3rd segment, respectively. There is a node in the 1st segment, and it broadcasts a B in the first time-slot. Other nodes in the 2nd segment and the 3rd segment sense the B, and drop out of the partition. The node broadcasting the B in the first iteration enters the second iteration. Then the 1st segment in the 1st iteration is split into three segments by the circles labeled with 1.1 and 1.2. Because the node only in the 2nd segment of the 2nd iteration, a B is sent by the node in the 2nd time-slot to notify other nodes. Finally, the node chooses a back-off timer randomly, and is selected as the relay-node at the cost of 3 time-slots. To improve the PDR in the dense network, the contention phase is allowed to attempt for N_{recon} times, and the exponential back-off timer is applied in our relay-node selection. The maximum width $C_w(c)$ of the exponential back-off timer in the c-th contention can be obtained as

$$C_w(c) = 2^{(c-1)} \cdot C_w(1). \quad (2)$$

Moreover, the protocol of Exponent-Based Partitioning Broadcast Protocol (EPBP) in our earlier work [11] is applied to proceed the channel access and the data transmission. And the mini-black-burst-assisted mechanism (mini-BBM) in [12] is adopted to reduce the partition latency.

IV. COMPLETE RELAY-NODE SELECTION ON THE CURVE ROAD

It can be found that the message maybe can not cover all the nodes on the road when the relay-nodes are selected only in the direction of the message dissemination. For example,

if the road section between P_C and P_D in Figure 1 is reshaped to the shape in Figure 3, the road section between P_G and P_H in Figure 3 is not only out of the communication range of the sender but also out of the communication range of the relay-node. In some scenes, e.g., for the safety-related message broadcast, the purpose of the relay-node selection is to disseminate the message as fast as possible, meanwhile to cover all the nodes on the road. Thus, a complete relay-node selection method that can cover every node on the road is expected.

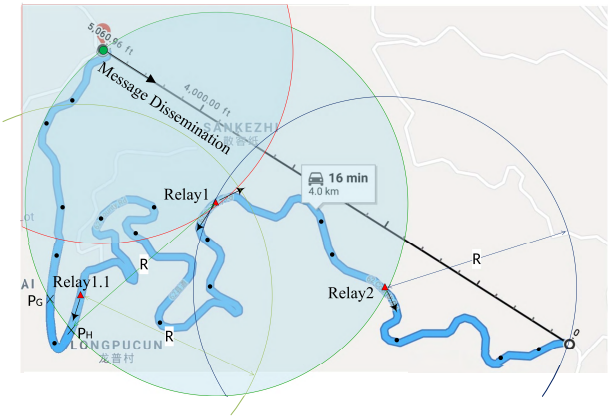

FIGURE 3. Procedure of the complete relay-node selection on curve road.

Figure 3 examples a complete relay-node selection method. The road area between P_G and P_H is out of the merged coverage of the sender and the relay-node (marked with the blue shadow in Figure 3), and is called a *vacant area*. When a relay-node learns that there is a vacant area on the road between the sender and itself, the relay-node initiates a *double-direction relay-node selection*. In the double-direction relay-node selection, the relay-node works as a new sender, and broadcasts a RTB package to initiate two relay-node selections in the message-dissemination direction and in the reverse direction simultaneously. The new sender is referred as the *bi-directional sender*, and the sender before the bi-directional sender is referred as the *original sender*. The selection in the direction of the message dissemination goes on with same procedure described in the above sections. And the selection in the reverse direction (referred as the *reverse selection*) is the same except the determination of the P_{opt}. The one that is closest to the bi-directional sender among the end points of these vacant areas is signed as a P_{opt} for the reverse selection. In the example of Figure 3, when Relay1 works as the sender and initiates the double-direction relay-node selection, the P_{opt} for the reverse selection is at P_H. If the reverse selection succeeds, the new relay-node (e.g., Relay1.1 in Figure 3) just starts the reverse selection in the direction to the original sender. And the reverse selection continues until all vacant areas are covered.

From the design of the double-direction relay-node selection, it can be known that the RTB package for the reverse selections also includes the locations of both the original sender and the bi-directional sender, so that the nodes in the reverse selection can obtain the P_{opt}. For example, the RTB package that Relay1.1 sends involves the locations of the original sender at Start and Relay1. Thus, from these location informations and its own location, the new relay-node can decide the P_{opt} for the next reverse selection and terminate the reverse selection or not. To initiate the three types of the relay-node selection (i.e., the traditional relay-node selection, the double-direction relay-node selection and the reverse selection), a RTB symbol is contained in the RTB package. We set the value of the RTB symbol as 0 for the traditional relay-node selection, 1 and 2 for the double-direction relay-node selection and the reverse selection, respectively. If a RTB package with a RTB symbol as 0 is received, the nodes in the message-dissemination direction mark the furthest junction of R_{sender} and the road as the P_{opt}, and conduct the traditional relay-node selection. If the RTB symbol is 1, the nodes in both directions join in the double-direction relay-node selection. The P_{opt} is set as the furthest junction by the nodes in the message-dissemination direction, and the nearest end point of the vacant area to the bi-directional sender is marked as the P_{opt} for the nodes in the reverse direction. And if the RTB symbol is 2, the nodes only in the reverse direction participate the reverse selection, and mark the next end point of the vacant area as the P_{opt}.

Moreover, to avoid the interference between the nodes in different direction selections, two different frequencies are allocated for Bs of the two direction selections.

In the example of Figure 3, the message transmitted from the Start is expected to cover the road area marked with the blue shadow from the Start to the point of End, and the first sender is located at the Start. In the first hop, Relay1 is selected. It finds there is a vacant area between the sender and itself with the aid of the GIS and GPS, then Relay1 works as the bi-directional sender and originates the double-direction relay-node selection. The locations of the sender (i.e., the original sender) and Relay1 (i.e.,the bi-directional sender) are included in the RTB package that Relay1 broadcasts, and the RTB symbol is assigned as 1. The nodes in the communication range of Relay1 receive the RTB package, and know that the selection in this hop is the double-direction relay-node selection from the RTB symbol. Then the nodes in the direction of the message dissemination compute the P_{opt} with the locations of Relay1 in the RTB package and the equipped GIS service. The P_{opt} is determined as the junction of the road and the R_{Relay1}, i.e., P_F. Whereas, the nodes in the reverse direction decide the P_{opt} at P_H with the help of the locations of the bi-directional sender and the original sender in the RTB package. Relay2 is selected in the message-dissemination direction, and a new RTB package is broadcast by Relay2. The RTB symbol of the new RTB package is set as 0 since no vacant area between Relay1 and Relay2. In the reverse direction, Relay1.1 is chosen, and the vacant area between P_H and P_G is covered by Relay1.1. If Relay1.1 derives that a vacant area exists between the original sender and itself, a RTB package with the RTB symbol of 2 is broadcast to start

the reverse selection. However, in this example, no vacant area exists, thus the selection in the reverse direction terminates.

In the procedure of the complete relay-node selection, the design for the location of P_{opt} in the reverse selection at the end point of the vacant area closest to the bi-directional sender or the sender of the reverse selection is to assure that each vacant area can be covered. The flow diagram of the complete relay-node selection is shown in Figure 4.

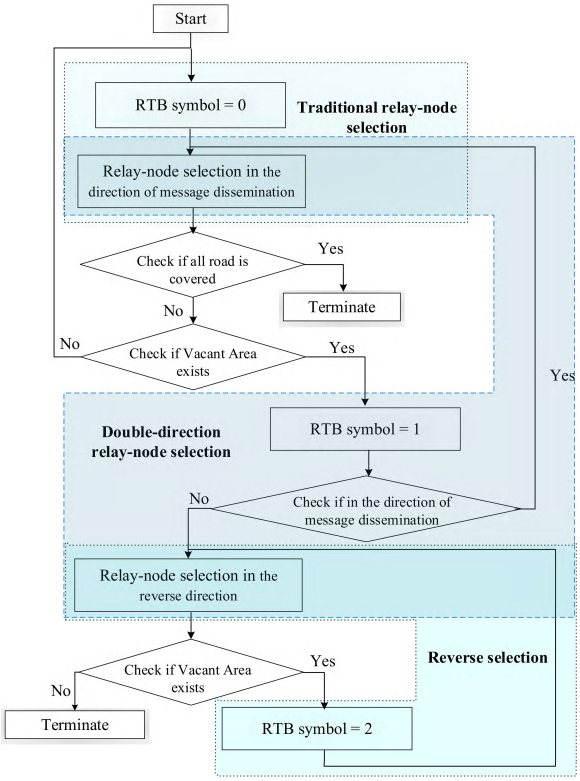

FIGURE 4. Flow diagram of the complete relay-node selection.

V. MODELING AND ANALYSIS

In this section, we define a metric of *Curving Rate* to measure the effect of the vehicle density on the performance of the relay-node selection on the curve road. Based on the definition of the curving rate, the performances of our proposal in terms of message dissemination speed and PDR are analyzed, and the closed-form expressions for these performances are derived.

A. DEFINITION OF METRICS

- **Curving rate** γ: is the ratio of the road length in the partition range R_p (i.e., the common range of R_{sender} and $R_{P_{opt}}$) and R. For example, shown in Figure 1, γ for the relay-node selection of the original sender can be computed as

$$\gamma = \frac{\left(L_{\text{Start},P_A} + L_{P_B,P_C} + L_{P_D,P_E} + L_{P_F,P_{opt}}\right)}{R}, \quad (3)$$

where $L_{A,B}$ represents the length of the road section between A and B.

- **Message progress** β: is the message dissemination distance normalized by the maximum dissemination distance. On the curve road, the maximum dissemination distance in one hop is defined as the length of the road from the sender to P_{opt}. Note that the message dissemination distance means the length of the road from the sender to the relay-node. β is defined as

$$\beta = \frac{L_{\text{Sender,Relay}}}{L_{\text{Sender},P_{opt}}}. \quad (4)$$

- **Message dissemination speed** v: is the ratio of the message dissemination distance $L_{\text{Sender,Relay}}$ and the one-hop delay T_d. Based on the definition of β, v can be defined as

$$v = \frac{L_{\max}\beta}{T_d}, \quad (5)$$

where $L_{\max}$ is the maximum message dissemination distance. In the case of the relay-node selection on the curve road, $L_{\max} = L_{\text{Sender},P_{opt}}$.

- **One-hop delay** T_d: is the delay that the message is transmitted from the sender to the relay-node. It is exactly defined as the duration from the instant that the node carrying the message prepares to access the channel to the instant that the message is received successfully by the relay-node. In our proposal, T_d consists of the initial latency T_{init} (i.e., the duration for the sender to access the channel), the partitioning latency T_{part}, the contention latency T_{cont} and the message transmission latency T_{data}. T_d is given as

$$T_d = T_{\text{init}} + T_{\text{part}} + T_{\text{cont}} + T_{\text{data}}. \quad (6)$$

- **Packet Delivery Ratio (PDR)**: is the number of packets received by the relay node successfully over the whole number of packets sent by the source node in one hop or multi-hop.

In the following subsection, we focus on the model for the performances in terms of T_{part}, T_{cont}, β and PDR, which are influenced by the design of our proposal.

B. PARTITION LATENCY

The vehicles are distributed on the road following Poisson distribution [7], [8], [10], and the probability of the vehicle number X on the road of the length l is given as

$$P_\mu(X = n) = \frac{e^{-\mu}\mu^n}{n!}, \quad (7)$$

where $\mu = \lambda l$ is the average vehicle number on the road, and λ is the vehicle density (vehicle per meter). Based on the definition of γ, the average vehicle number in the partition range can be derived as

$$\mu_{\text{p\_range}} = \lambda\gamma R, \quad (8)$$

and the average vehicle number in the k-th segment of the j-th iteration is derived as

$$\mu_{\text{seg}}^{j,k} = \lambda \gamma_{\text{seg}}^{j,k} W_{\text{seg}}(j,k), \tag{9}$$

where $\gamma_{\text{seg}}^{j,k}$ represents the curving rate in the k-th segment of the j-th iteration. Thus, the probability of the selection of the k-th segment in the j-th iteration can be given as

$$\begin{aligned} P_{\text{seg\_sel}}^{j,k} &= \mathrm{P}_{\mu_{\text{seg\_bro}}^{j,k}}(X=0)\left(1-\mathrm{P}_{\mu_{\text{seg}}^{j,k}}(X=0)\right) \\ &= e^{-\mu_{\text{seg\_bro}}^{j,k}}\left(1-e^{-\mu_{\text{seg}}^{j,k}}\right), \end{aligned} \tag{10}$$

where $\mu_{\text{seg\_bro}}^{j,k}$ is the average vehicle number in other segments for the k-th segment in the message broadcasting direction, which can be attained as $\mu_{\text{seg\_bro}}^{j,k} = \sum_{n=1}^{k-1} \mu_{\text{seg}}^{j,n}$.

From (9) and (10), it can be seen that the influence of the shape of the curve road on the performance of the relay-node selection is measured with the metric γ.

Based on the above results, the average duration T_{part} spent during the partitioning phase can be obtained as

$$T_{\text{part}} = \left(\left(\sum_{j=1}^{N_{\text{iter}}}\sum_{k=1}^{(N_{\text{part}})^j}\left(N_{\text{p\_slot}}(k)P_{\text{seg\_sel}}^{j,k}\right)\right)+1\right)T_{\text{slot}}, \tag{11}$$

where $N_{\text{p\_slot}}(k)$ is the number of time slots spent when the k-th segment is selected. $N_{\text{p\_slot}}(k)$ can be given as

$$N_{\text{p\_slot}}(k) = \begin{cases} k \bmod N_{\text{part}}, & \text{if } (k \bmod N_{\text{part}}) < N_{\text{part}} \\ N_{\text{part}} - 1, & \text{if } (k \bmod N_{\text{part}}) = N_{\text{part}} \end{cases} \tag{12}$$

C. CONTENTION LATENCY

Since the CTB-contention occurs in the nonempty segment, only the success case and the collision case exist in the contention phase. Following a similar procedure in [12], the single probabilities of the success case and the collision case in the c-th contention of the k-th final segment can be derived as

$$p_{\text{suc\_con}}^{k,c} = \frac{\mu_k p_c e^{-\mu_k p_c}}{1-e^{-\mu_k p_c}}, \tag{13}$$

$$p_{\text{col\_con}}^{k,c} = 1 - \frac{\mu_k p_c e^{-\mu_k p_c}}{1-e^{-\mu_k p_c}}, \tag{14}$$

where $\mu_k = \mu_{\text{seg}}^{N_{\text{iter}},k}$ is the average number of vehicles in the k-th final segment for simplicity, and $p_c = \frac{1}{C_{\text{w}}(c)}$. So, the whole success probability after c contentions in the k-th final segment is computed as

$$p_{\text{suc}}^{k,c} = p_{\text{suc\_con}}^{k,c}\prod_{l=0}^{c-1} p_{\text{col\_con}}^{k,l}, \tag{15}$$

where $p_{\text{col\_con}}^{k,0} = 1$ and $c = 1, 2, \cdots$. The whole contention latency $T_{\text{con\_seg}}^{k}$ of the k-th segment can be derived as

$$T_{\text{con\_seg}}^{k} = \sum_{c=1}^{\infty} p_{\text{suc}}^{k,c}\left(\sum_{l=0}^{c-1} T_{\text{col}}(l) + T_{\text{suc}}(c)\right), \tag{16}$$

where $T_{\text{col}}(c)$ and $T_{\text{suc}}(c)$ are the duration spent in the collision or the success case of the c-th contention, respectively. Finally, the average contention latency in the contention phase can be computed as

$$T_{\text{con}} = \sum_{k=1}^{N_{\text{part}}^{N_{\text{iter}}}} T_{\text{con\_seg}}^{k} P_{\text{seg\_sel}}^{k}, \tag{17}$$

where $P_{\text{seg\_sel}}^{k} = P_{\text{seg\_sel}}^{N_{\text{iter}},k}$ is the probability that the k-th segment is selected as the final segment in the last iteration.

D. MESSAGE PROGRESS

One-hop message progress β is calculated as

$$\beta = \sum_{k=1}^{(N_{\text{part}})^{N_{\text{iter}}}} M_k P_{\text{seg\_sel}}^{k}, \tag{18}$$

where M_k is the average message progress if the k-th segment is the final segment. And M_k can be given by

$$\begin{aligned} M_k = \frac{1}{\gamma}\Big[&\frac{W_{\text{seg}}(N_{\text{iter}},k)\gamma_{\text{seg}}^{N_{\text{iter}},k})}{2} \\ &+ \sum_{s=k+1}^{(N_{\text{part}})^{N_{\text{iter}}}}\left(W_{\text{seg}}(N_{\text{iter}},s)\right)\Big]. \end{aligned} \tag{19}$$

E. PDR

In this analysis, since the focus of this paper is the relay selection in MAC layer, we only consider the relay selection failure caused by the CTB-contention attempt over the pre-assigned threshold N_{recon}. So the probability of the selection failure in the k-th final segment is

$$p_{\text{fail\_seg}}^{k} = \prod_{c=1}^{N_{\text{recon}}} p_{\text{col\_con}}^{k,c}. \tag{20}$$

The probability of the selection failure in one hop is

$$P_{\text{fail}} = \sum_{k=1}^{(N_{\text{part}})^{N_{\text{iter}}}}\left(p_{\text{fail\_seg}}^{k} P_{\text{seg\_sel}}^{k}\right). \tag{21}$$

So the PDR in one hop can be attained as

$$PDR = 1 - P_{\text{fail}}. \tag{22}$$

VI. RESULTS AND ANALYSIS

In this section, the simulation is conducted on a real-world typical mountain road to validate the models for the performances of our proposal and prove the effectiveness of our proposal on the curve road.

A. INTRODUCTION OF EVALUATION

To evaluate the complete relay-node selection, the revised mountain road with the length of 4 kilometers in Ziquejie Park, China shown in Figure 3, is adopted as the simulation scenario. The curve road is 2-lane dual driveway and is full of sharp turns. The message is expected to be delivered from

Start to End, and to cover the curve road marked in blue. Vehicles locate on the road according to Poison Distribution, and move at fixed velocity without lane change and overtaking. The velocity for every vehicle is set randomly following a uniform distribution in $[\frac{1}{2}v_{\max}, v_{\max}]$, and $v_{\max}$ is the maximum speed for vehicle related to the safety inter-vehicle distance [24], [25], which is determined as

$$v_{\max} = min(d_{\text{inter\_veh}}, v_{\max\_\text{rule}}), \tag{23}$$

where $d_{\text{inter\_veh}}$ is the average inter-vehicle distance, and $v_{\max\_\text{rule}}$ represents the limit speed in a specific road scenario. The units of $v_{\max\_\text{rule}}$ and $d_{\text{inter\_veh}}$ are km/h and meter, respectively. The $v_{\max\_\text{rule}}$ in the simulation is set as 40 km/h according to [25]. To test and verify the performance in sparse networks and dense networks, the vehicle density for simulation varies from 0.005 to 0.305 vehicle/meter. The choice of the density range means that at least one node in the partition range at the lowest density and that the average distance is 7 meters between two adjacent vehicles at the highest density when the communication range is set as 500 meters in the simulation. The VANET environment is simulated in MATLAB. Our earlier research [12], [13] and the conclusion in [26] and [27] point out that the vehicle movement has a minor influence on the relay-node selection. Moreover, the results shown in Figure 12 indicate the one-hop delay for all examined method is less than 1.83 ms, and a vehicle with a velocity of 40 m/s just move for a distance of 0.072 meter. So we think that the set of the vehicle movement and the selection of MATLAB are acceptable.

The pre-assigned thresholds N_{recon} for the contention re-attempt N_{recon} is set to 3. The arrival rate of messages is set to 2 EMs/s. Other major communication parameters adopted in the simulation are listed in Table. 2, which are identical to those used in [8], [12], and [13].

TABLE 2. Major communication parameters.

Parameters	Default values
Bit Rate	18Mbps
Message Packet Size	500Bytes
RTB Packet Size	20 Bytes
CTB Packet Size	14 Bytes
Slot Time	13 μs
DIFS	58 μs
SIFS	32 μs
Transceiver's Switching Time	1 μs
Communication Range	500m
Confidence Interval	95%

Due to the ergodic theorem [28], we performed sufficient repetitions of Monte Carlo simulation [3] for statistical significance, 2000 repetitions are for all results. These outcomes are averaged to produce the graphs presented in this section with 95% confidence intervals. The confidence intervals are marked with the error bars in the plots.

B. MODEL VALIDATION

In this subsection, we conduct the simulation with a varied parameter of N_{iter}, N_{part} and A on two road sections, shown in Figure 5. The two road sections are highlighted in yellow from S_1 to E_1 and from S_2 to E_2, respectively. The two sections are in the coverage of the senders which at S_1 or S_2, and the curving rate γ for them are significantly different, i.e., 4.9223 and 1.8128, respectively. For distinguish, the choice of N_{iter}, N_{part} and A is a small value.

FIGURE 5. Simulation scenarios for model validation.

As shown in Figures 6 to 9, the results of the simulation coincide the analytic results. It proves the validation of the models.

Moreover, it is observed that the choice of a larger value for these parameters of N_{iter}, N_{part} and A can lead to a smaller partition latency, a larger contention latency, a higher message progress and a better PDR. And with the increasing of the vehicle density, the partition latency decreases, as well as the contention latency, message progress and PDR rise. The tendencies are the same to that when the exponent partition method is applied in the scenarios of the straight road and the intersection. However, some differences are noticed. In Figure 8, at the lowest vehicle density of 0.005 vehicle/meter, the order of the message progress from the smallest to the largest is not expected. For example, in Figure 8(a), at the other vehicle densities the message progress goes up with the increasing of A. Whereas, at 0.005 vehicle/meter, the message progress for $A = 2$ is the largest, and that for $A = 32$ is the smallest. The reason is that the final segment for the smaller A may be closer to P_{opt}. Figure 5 examples the application of the exponent partition with $A = 0.1$ and $A = 2$ at the same $(N_{iter}, N_{part}) = (1, 3)$. The solid circles correspond the partition for $A = 0.1$, and the dashed circles for $A = 2$. In the example, only one node in the R_p at the low density. The final segment for $A = 0.1$ is on the road section between the circles marked by 1.1 and 1.2, and the final segment for $A = 2$ between the circles marked by 1 and 2.1. It is observed that the possible location for the relay node closest to P_{opt} for $A = 0.1$ is P_L, and that for $A = 2$ is P_M in Figure 5. The same event may happen at the varied N_{iter} and N_{part} in the sparse networks. Therefore, it can be derived that at the low vehicle density the smaller values for N_{iter}, N_{part} and A can bring up a higher message progress since the shape of the curve road is irregular.

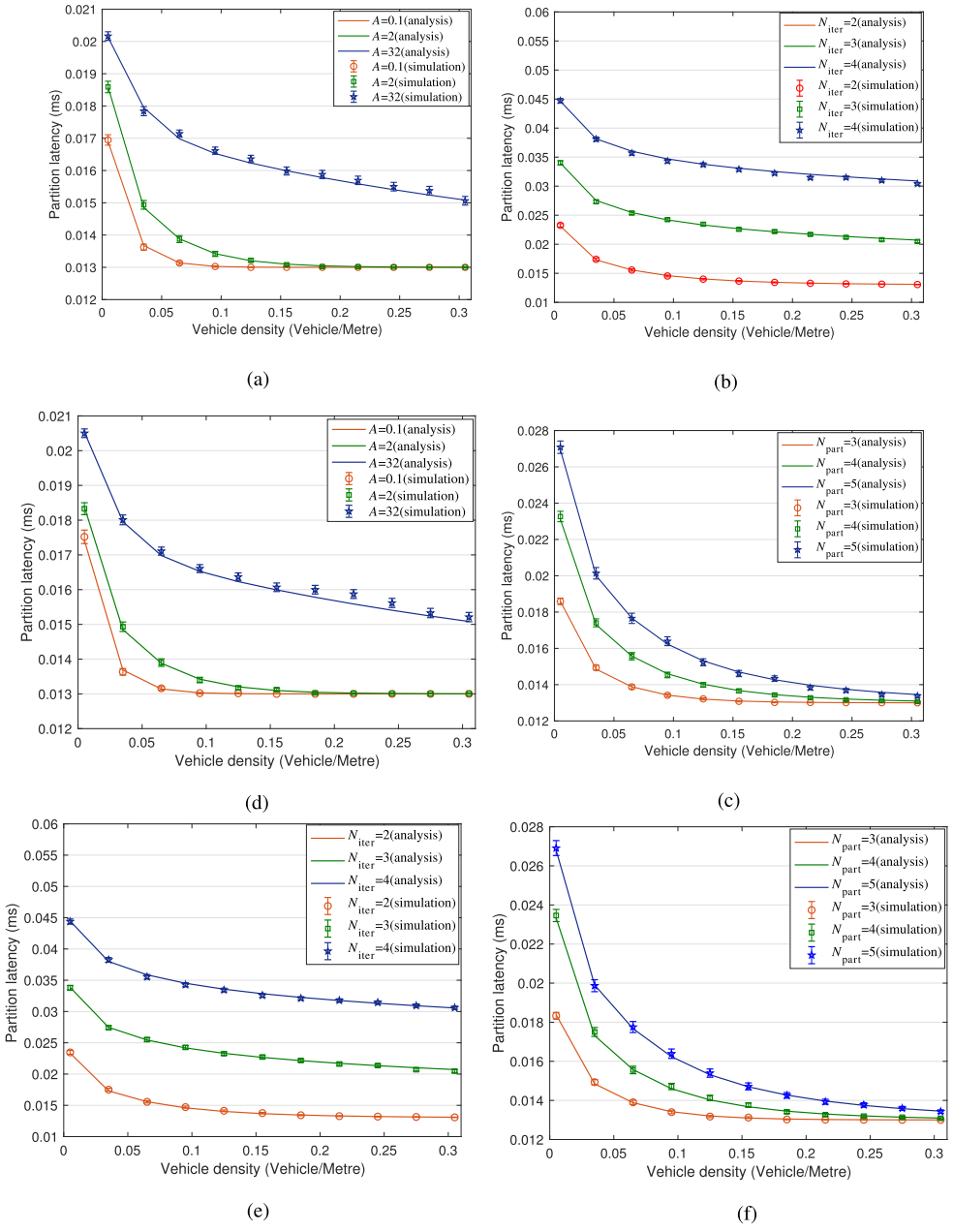

FIGURE 6. Validation of the model for partition latency. (a) When $(N_{\text{iter}}, N_{\text{part}}) = (2, 4)$ on Section 1. (b) When $(N_{\text{part}}, A) = (4, 2)$ on Section 1. (c) When $(N_{\text{iter}}, A) = (2, 2)$ on Section 1. (d) When $(N_{\text{iter}}, N_{\text{part}}) = (2, 4)$ on Section 2. (e) When $(N_{\text{part}}, A) = (4, 2)$ on Section 2. (e) When $(N_{\text{iter}}, A) = (2, 2)$ on Section 2.

C. PERFORMANCE VALUATION

To evaluate the effectiveness and the improvement of our proposal on the curve road, we simulated our proposal and the adapted methods that are based on the mentioned methods, i.e., PMBP, BPAB and 3P3B. These methods are adapted to be suitable on the curve road and are combined in the proposed complete relay-node selection. The selections of N_{iter} for BPAB and 3P3B are set as 3 and 2 according to [8], and that for PMBP is 10. In our proposal, $(N_{\text{iter}}, N_{\text{part}}, A) = (2, 4, 2)$ according to [12]. Moreover, to evaluate the gains benefited from the exponent partition and the mini-BBM [12], an iterative-partition-based method with equal segments and the Complete without mini-BBM are simulated. $(N_{\text{iter}}, N_{\text{part}})$ for the method with equal segments is set as $(2, 4)$ as same as that in the Complete, and is referred as IPES24. For fairness, the exponential back-off timer is applied in all examined methods, and $C_{\text{w}}(1) = 4$ for all.

Figure 10 shows the partition latency of all examined relay-node selection methods against the vehicle density. It can be observed that the partition latency of BPAB keeps a constant value, and that of Robust, IPES24 and 3P3B fall at first and then approximate some constant values with the rising of the

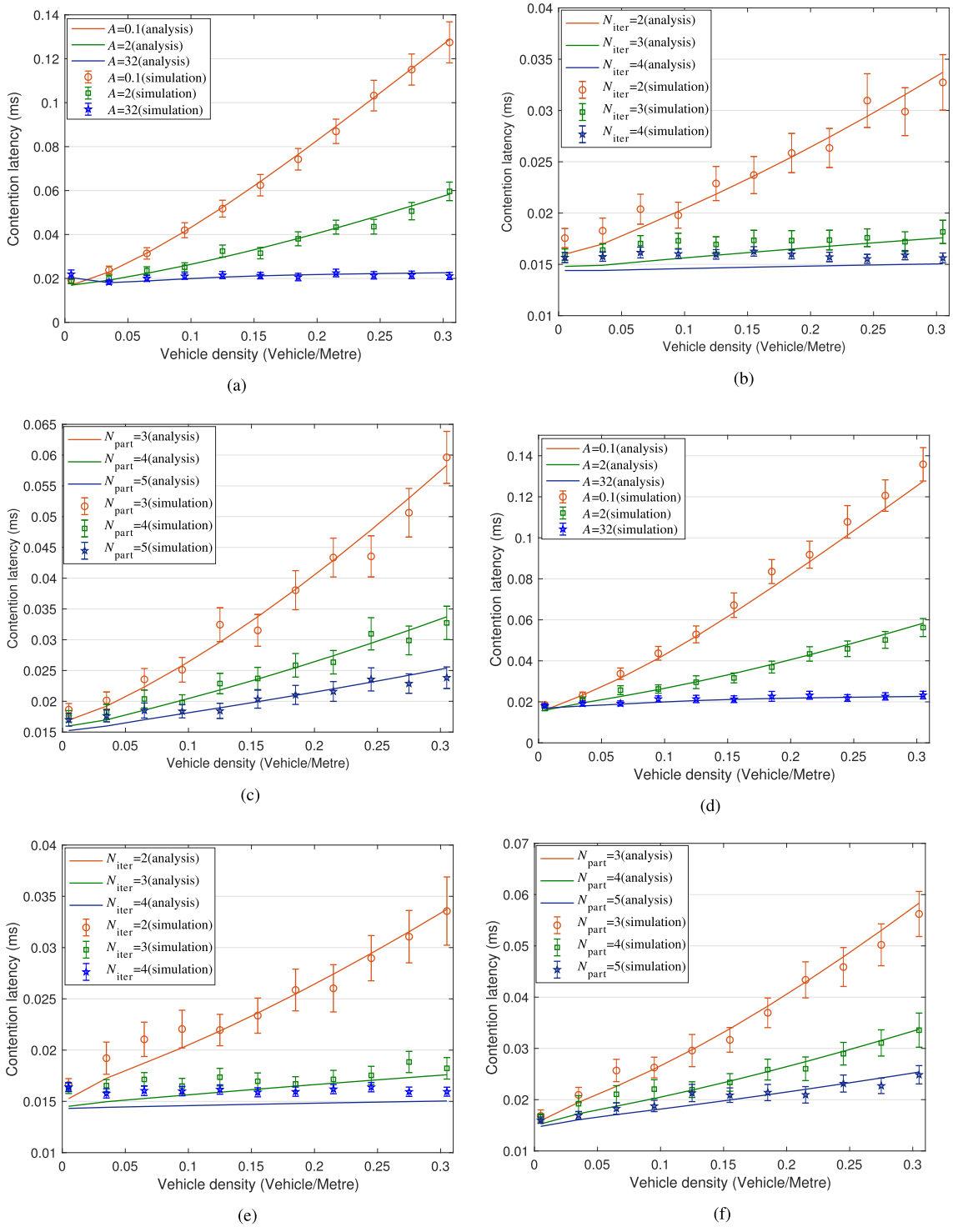

FIGURE 7. Validation of the model for contention latency. (a) When $(N_{\text{iter}}, N_{\text{part}}) = (2, 4)$ on Section 1. (b) When $(N_{\text{part}}, A) = (4, 2)$ on Section 1. (c) When $(N_{\text{iter}}, A) = (2, 2)$ on Section 1. (d) When $(N_{\text{iter}}, N_{\text{part}}) = (2, 4)$ on Section 2. (e) When $(N_{\text{part}}, A) = (4, 2)$ on Section 2. (f) When $(N_{\text{iter}}, A) = (2, 2)$ on Section 2.

density, whereas that of PMBP goes up and becomes steady. The reason lies in that when the density becomes higher the node exists in the segment close to the P_{opt} more likely. Then the Complete, IPES24 and 3P3B cost less slots whereas PMBP costs more slots. And the number of slots spent for the whole partition procedure of BPAB is fixed as $N_{\text{iter}} - 1$. Though the Complete without mini-BBM performs worse than 3P3B and IPES24, the Complete attains an improvement of more than 55.385% in terms of the partition latency than 3P3B and IPES24 with the mini-BBM applied.

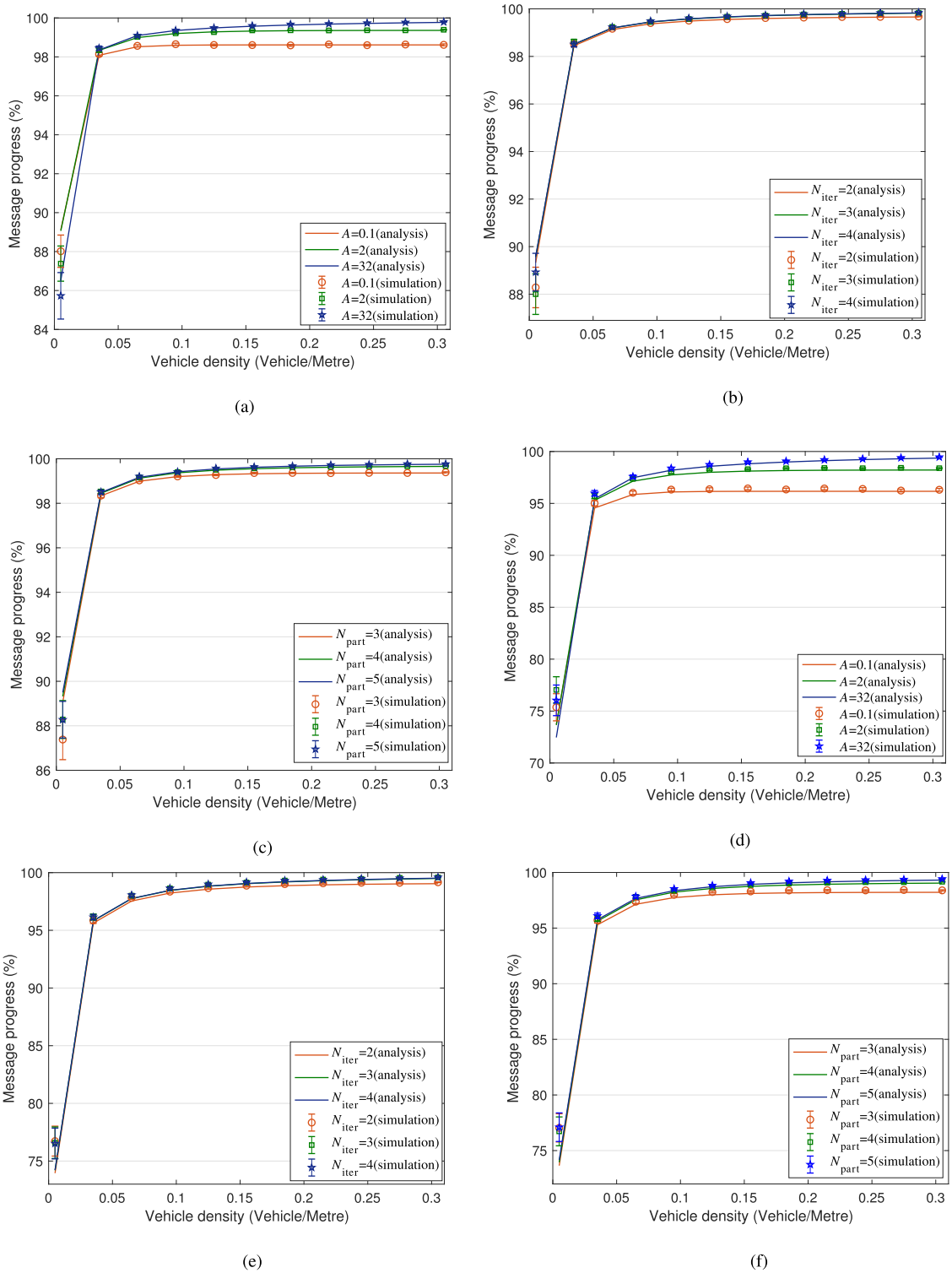

FIGURE 8. Validation of the model for message progress. (a) When $(N_{\text{iter}}, N_{\text{part}}) = (2, 4)$ on Section 1. (b) When $(N_{\text{part}}, A) = (4, 2)$ on Section 1. (c) When $(N_{\text{iter}}, A) = (2, 2)$ on Section 1. (d) When $(N_{\text{iter}}, N_{\text{part}}) = (2, 4)$ on Section 2. (e) When $(N_{\text{part}}, A) = (4, 2)$ on Section 2. (f) When $(N_{\text{iter}}, A) = (2, 2)$ on Section 2.

Figure 11 exhibits that the contention latency of all methods. All contention latency increase as the vehicle density becomes heavier, since more nodes enter the CTB-contention in the heavier traffic. Among these methods, the Complete performs the best which is improved by more than 82.41%, 81.62% and 71.62% than BPAB, 3P3B and IPES24 at the high density of 0.305 vehicle/meter respectively and 35.34% than PMBP at the low density of 0.005 vehicle/meter.

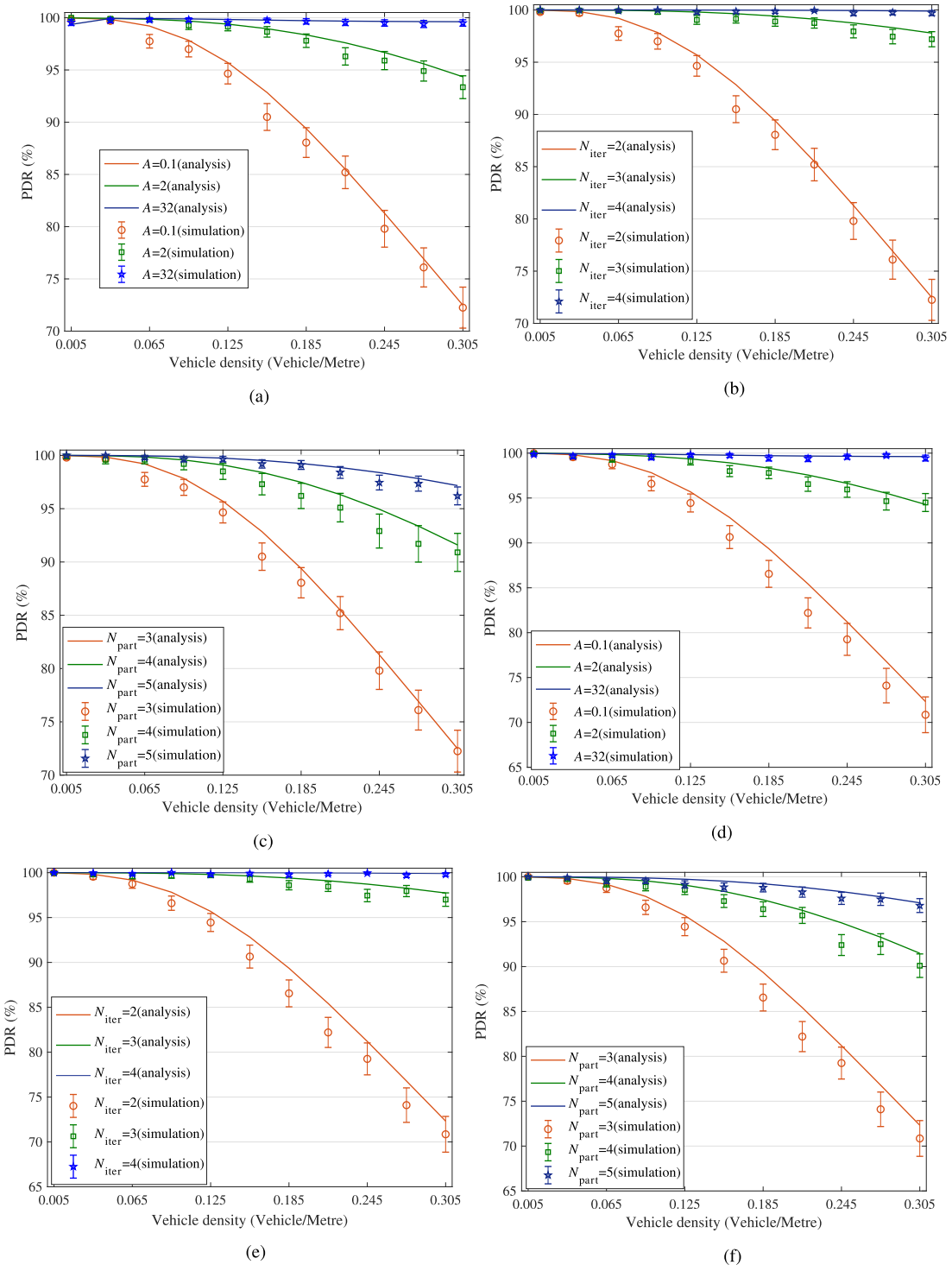

FIGURE 9. Validation of the model for PDR. (a) When $(N_{\text{iter}}, N_{\text{part}}) = (2, 3)$ on Section 1. (b) When $(N_{\text{part}}, A) = (3, 0.1)$ on Section 1. (c) When $(N_{\text{iter}}, A) = (2, 0.1)$ on Section 1. (d) When $(N_{\text{iter}}, N_{\text{part}}) = (2, 3)$ on Section 2. (e) When $(N_{\text{part}}, A) = (4, 2)$ on Section 2. (f) When $(N_{\text{iter}}, A) = (2, 2)$ on Section 2.

The gap between the curves corresponding the IPES24 and the Complete shows the significant gain specially at the heavy density benefited from the exponent partition method.

Contributed from the gains in the partition latency and the contention latency, the Complete method performs the best in terms of one-hop delay among all methods, shown in Figure 12. Moreover, the one-hop delay of the Complete gives the stablest presentation. It is the most abstracting advantage for the Complete method.

In the iterative-partition-based relay-node selection, the width of the final segment decides the message progress. Thus, shown in Figure 13 the Complete presents the

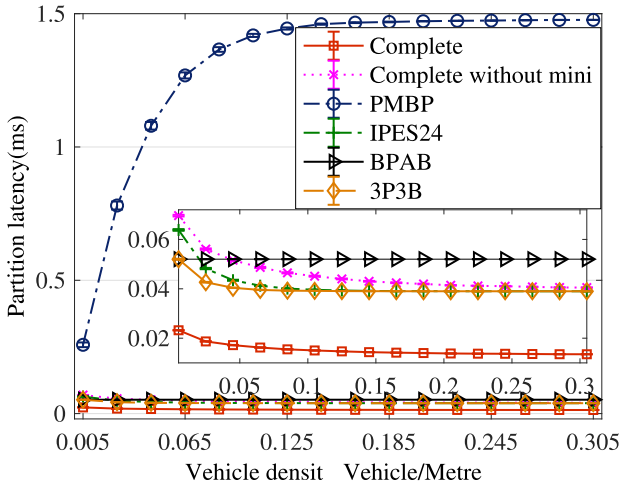

FIGURE 10. Performance comparison in terms of partition latency.

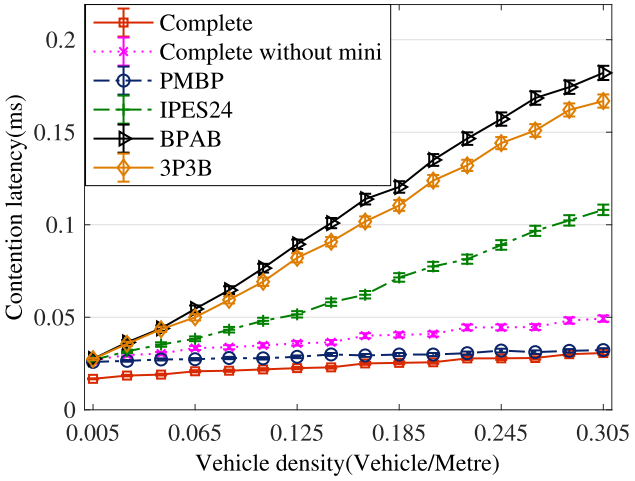

FIGURE 11. Performance comparison in terms of contention latency.

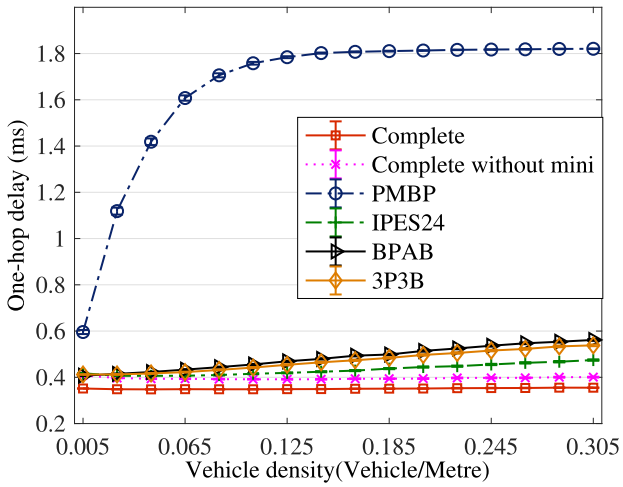

FIGURE 12. Performance comparison in terms of one-hop delay.

second best performance in terms of the message progress, and performs just worse than the best performing PMBP by no more than 0.21%. It is benefited from the exponent

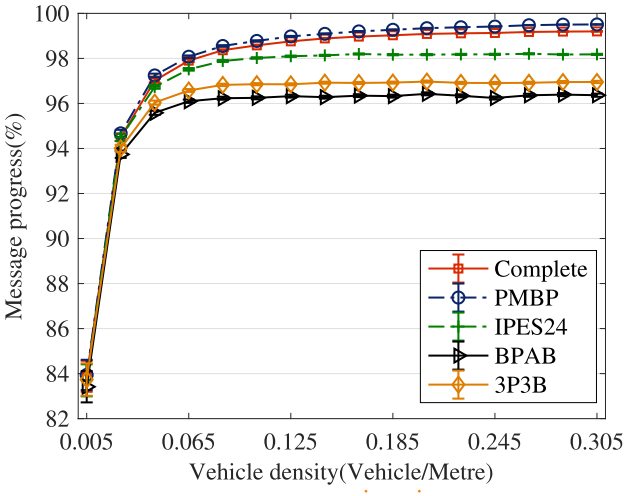

FIGURE 13. Performance comparison in terms of message progress.

partition method, which can be illustrated by the cueves of the IPES24 and the Complete in Figure 13.

Figure 14 shows the performance of all examined methods in terms of the message dissemination speed. Due to the outstanding performances in terms of the one-hop delay and the message progress, the Complete outperforms IPES24, 3P3B, BPAB and PMBP by at least 16.20%, 17.40%, 16.18% and 28.05%. Furthermore, the gains compared with IPES24, 3P3B, BPAB and PMBP in the high density of 0.305 vehicle/meter are 31.99%, 49.90%, 56.19% and 414.92%, respectively. The gain due to the mini-BBM corresponds the gap between the curve lines of the Complete and the Complete without mini-BBM. Similarly, the gain contributed by the exponent partition corresponds the gap between the curve lines of the Complete without mini-BBM and IPES24. Note that the IPES24 outperforms 3P3B, and this is inconsistent with the result in [8]. It is because that the exponential back-off timer is applied in all examined methods

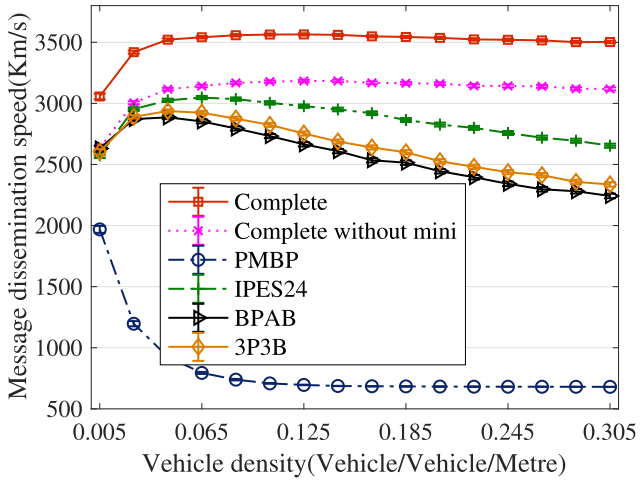

FIGURE 14. Performance comparison in terms of message dissemination speed.

and the scenarios in our paper and [8] are different, i.e., the curve road and the straight road.

The number of nodes in the CTB-contention determines the performance in terms of PDR. Thus, shown from Figure 15, the Complete performs the second best, and the performance gap between the Complete and the best performing PMBP is slight. The improvements of the Complete compared with IPES24, 3P3B and BPAB boom with the increasing of the vehicle density. At the high density of 0.305 vehicle/meter, the gains are 5.56%, 24.16% and 36.02%, respectively. Under the simulation conditions, the performance of the Complete in terms of PDR is over 99.7%.

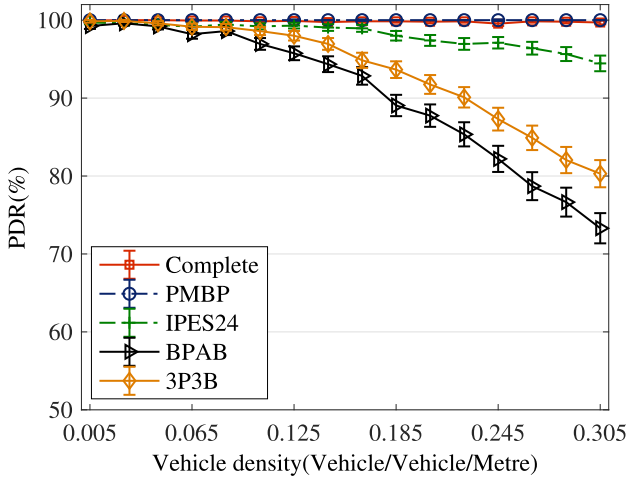

FIGURE 15. Performance comparison in terms of PDR.

VII. CONCLUSION

In this paper, we propose the complete relay-node selection method on the curve road. To the best of our knowledge, it is the first time to develop the relay-node selection on the curve road. Through the definitions of the optimal position and the partition range, the exponent partition is adapted for the application of the relay-node selection on the curve road to deliver the message along the road as fast as possible. And the double-direction relay-node selection and the reverse selection are designed to assure that all area in the road can be covered. Moreover, we define the metric of the curving rate to describe the bending degree of the curve road quantitatively, and construct the model of the performances for our proposed relay-node selection in terms of the message dissemination speed and PDR. The simulation on the realistic mountain road is conducted. The simulation results validate the models and evaluate the significant performances of the complete relay-node selection method. Furthermore, the method can be adapted in the routing design [15], [29]–[32]. For example, in [15], P_{opt} is located at the road curving to achieve the best wireless quality.

In the future, we will extend our works to the relay-node selection on the 3-dimension structure of the road and the adaptive selection of the relay-node on different structures of the road.

ACKNOWLEDGMENT

The authors would like to thank the reviewers and all people for their helpful comments and valuable efforts to improve the paper.

REFERENCES

[1] *Study on Enhancement of 3GPP Support for 5G V2X Services*, document 3GPP TR 22.886, v.15.1.0, 2017.

[2] K. Zhang, S. Leng, Y. He, S. Maharjan, and Y. Zhang, "Cooperative content caching in 5G networks with mobile edge computing," *IEEE Wireless Commun.*, vol. 25, no. 3, pp. 80–87, Jun. 2018.

[3] K. Zhang, Y. Mao, S. Leng, Y. He, and Y. Zhang, "Mobile-edge computing for vehicular networks: A promising network paradigm with predictive offloading," *IEEE Veh. Technol. Mag.*, vol. 12, no. 2, pp. 36–44, Jun. 2017.

[4] K. Zheng, Q. Zheng, P. Chatzimisios, W. Xiang, and Y. Zhou, "Heterogeneous vehicular networking: A survey on architecture, challenges, and solutions," *IEEE Commun. Surveys Tuts.*, vol. 17, no. 4, pp. 2377–2396, 4th Quart., 2015.

[5] S. M. Hanshi, T.-C. Wan, M. M. Kadhum, and A. A. Bin-Salem, "Review of geographic forwarding strategies for inter-vehicular communications from mobility and environment perspectives," *Veh. Commun.*, vol. 14, pp. 64–79, Oct. 2016, doi: 10.1016/j.vehcom.2018.09.005.

[6] S. Boussoufa-Lahlah, F. Semchedine, and L. Bouallouche-Medjkoune, "Geographic routing protocols for vehicular ad hoc NETworks (VANETs): A survey," *Veh. Commun.*, vol. 11, pp. 20–31, Jan. 2018.

[7] Y. Bi, H. Zhao, and X. Shen, "A directional broadcast protocol for emergency message exchange in inter-vehicle communications," in *Proc. ICC*, Dresden, Germany, Jun. 2009, pp. 1–5.

[8] C. Suthaputchakun, M. Dianati, and Z. Sun, "Trinary partitioned black-burst-based broadcast protocol for time-critical emergency message dissemination in VANETs," *IEEE Trans. Veh. Technol.*, vol. 63, no. 6, pp. 2926–2940, Jul. 2014.

[9] G. Korkmaz, E. Ekici, and F. Ozguner, "Black-burst-based multihop broadcast protocols for vehicular networks," *IEEE Trans. Veh. Technol.*, vol. 56, no. 5, pp. 3159–3167, Sep. 2007.

[10] J. Sahoo, E. H. K. Wu, P. K. Sahu, and M. Gerla, "Binary-partition-assisted MAC-layer broadcast for emergency message dissemination in VANETs," *IEEE Trans. Intell. Transp. Syst.*, vol. 12, no. 3, pp. 757–770, Sep. 2011.

[11] D. Cao, Z. B. Lei, B. F. Ji, and C. G. Li, "Exponent-based partitioning broadcast protocol for emergency message dissemination in vehicular networks," *IEICE Trans. Fundam. Electron., Commun. Comput. Sci.*, vol. E99.A, no. 11, pp. 2075–2083, 2016.

[12] D. Cao, B. Zheng, B. Ji, Z. Lei, and C. Feng, "A robust distance-based relay selection for message dissemination in vehicular network," *Wireless Netw.*, pp. 1–17, Oct. 2018, doi: 10.1007/S11276-018-1863-4.

[13] D. Cao, B. Zheng, J. Wang, B. Ji, and C. Feng, "Design and analysis of a general relay-node selection mechanism on intersection in vehicular networks," *Sensors*, vol. 18, p. 4251, Dec. 2018. Accessed: Jan. 7, 2019, doi: 10.3390/s18124251.

[14] B. Karp and H.-T. Kung, "GPSR: Greedy perimeter stateless routing for wireless networks," in *Proc. 6th Annu. Int. Conf. Mobile Compu. Netw.*, Boston, MA, USA, Aug. 2000, pp. 243–254.

[15] C. Wu, S. Ohzahata, and T. Kato, "Fuzzy logic based multi-hop broadcast for high-density vehicular ad hoc networks," in *Proc. IEEE Veh. Netw. Conf.*, Dec. 2010, pp. 17–24.

[16] V. Naumov and T. R. Gross, "Connectivity-aware routing (CAR) in vehicular ad-hoc networks," in *Proc. 26th IEEE Int. Conf. on Comput. Commun.*, Anchorage, AK, USA, May 2007, pp. 1919–1927.

[17] J. Bernsen and D. Manivannan, "RIVER: A reliable inter-vehicular routing protocol for vehicular ad hoc networks," *Comput. Netw.*, vol. 52, no. 17, pp. 3795–3807, 2012.

[18] M. Noor-A-Rahim, G. G. M. N. Ali, H. Nguyen, and Y. L. Guan, "Performance analysis of IEEE 802.11p safety message broadcast with and without relaying at road intersection," *IEEE Access*, vol. 6, pp. 23786–23799, Apr. 2018.

[19] C. Li, H. J. Yang, F. Sun, J. M. Cioffi, and L. Yang, "Multiuser overhearing for cooperative two-way multiantenna relays," *IEEE Trans. Veh. Technol.*, vol. 65, no. 5, pp. 3796–3802, May 2016.

[20] X. M. Ma, X. Y. Yin, G. Butron, C. Penney, and K. S. Trivedi, "Packet delivery ratio in k-dimensional broadcast ad hoc networks," *IEEE Commun. Lett.*, vol. 17, no. 12, pp. 2252–2255, Dec. 2013.

[21] W. Li, X. Ma, J. Wu, K. S. Trivedi, X.-L. Huang, and Q. Liu, "Analytical model and performance evaluation of long-term evolution for vehicle safety services," *IEEE Trans. Veh. Technol.*, vol. 66, no. 3, pp. 1926–1939, Mar. 2017.
[22] C. Li, S. Zhang, P. Liu, F. Sun, J. M. Cioffi, and L. Yang, "Overhearing protocol design exploiting intercell interference in cooperative green networks," *IEEE Trans. Veh. Technol.*, vol. 65, no. 1, pp. 441–446, Jan. 2016.
[23] J. Mena, P. Bankole, and M. Gerla, "Multipath TCP on a VANET: A performance study," in *Proc. ACM SIGMETRICS*, Urbana, IL, USA, Jun. 2017, pp. 39–40.
[24] State of Virginia. *Tables of Speed and Stopping Distances*. Accessed: Dec. 10, 2018. [Online]. Available: https://law.lis.virginia.gov/vacode/46.2-880/
[25] *Regulations for the Implementation of the Road Traffic Safety Law in People's Republic of China*. Accessed: Dec. 10, 2018. [Online]. Available: http://www.gov.cn/zhengce/content/2008-03/
[26] X. Ma, J. Zhang, X. Yin, and K. S. Trivedi, "Design and analysis of a robust broadcast scheme for VANET safety-related services," *IEEE Trans. Veh. Technol.*, vol. 61, no. 1, pp. 46–61, Jan. 2012.
[27] C. Li, P. Liu, C. Zou, F. Sun, J. M. Cioffi, and L. Yang, "Spectral-efficient cellular communications with coexistent one- and two-hop transmissions," *IEEE Trans. Veh. Technol.*, vol. 65, no. 8, pp. 6765–6772, Aug. 2016.
[28] P. Del Moral, A. Doucet, and A. Jasra, "Sequential Monte Carlo samplers," *J. Roy. Stat. Soc. B (Stat. Methodol.)*, vol. 68, no. 3, pp. 411–436, 2006.
[29] Z. Liao, J. Liang, and C. Feng, "Mobile relay deployment in multihop relay networks," *Comput. Commun.*, vol. 112, pp. 14–21, Nov. 2017.
[30] E. B. Tirkolaee, A. A. R. Hosseinabadi, M. Soltani, A. K. Sangaiah, and J. Wang, "A hybrid genetic algorithm for multi-trip green capacitated arc routing problem in the scope of urban services," *Sustainability*, vol. 10, no. 5, pp. 1–21, 2018.
[31] J. Yao, K. Zhang, Y. Yang, and J. Wang, "Emergency vehicle route oriented signal coordinated control model with two-level programming," *Soft Comput.*, vol. 22, no. 13, pp. 4283–4294, 2018.
[32] J. Wang, C. Ju, Y. Gao, A. K. Sangaiah, and G.-J. Kim, "A PSO based energy efficient coverage control algorithm for wireless sensor networks," *Comput. Mater. Continua*, vol. 56, pp. 433–446, Sep. 2018.

DUN CAO received the B.S. degree in communication engineering from Central South University, China, in 2001, the M.S. degree in information systems and communications from Hunan University, China, in 2006, and the Ph.D. degree in vehicle engineering from the Changsha University of Science and Technology, China, in 2017, where she is currently a Faculty Member with the School of Computer and Communication Engineering. She was a Visiting Scholar with the National Mobile Communications Research Laboratory, Southeast University, China, from 2012 to 2013, and with The University of Texas at Arlington, from 2013 to 2017. Her research interests include vehicular networks and MIMO wireless communications.

YONGHE LIU received the B.S. and M.S. degrees from Tsinghua University, in 1998 and 1999, respectively, and the Ph.D. degree from Rice University, in 2004. He was with Texas Instruments for about two and half years. In 2004, he joined the Department of Computer Science and Engineering, The University of Texas at Arlington, where he is currently an Associate Professor. His research interests include networking, wireless systems, and their system prototyping.

XIAOMIN MA received the B.E. and M.E. degrees in electrical engineering, in 1984 and 1989, respectively, and the Ph.D. degree in information engineering from the Beijing University of Posts and Telecommunications, China, in 1999. From 2000 to 2002, he was a Postdoctoral Fellow with the Department of Electrical and Computer Engineering, Duke University, USA. He is currently a Professor with the School of Engineering, Oral Roberts University, USA. He has published one book and more than 110 papers in peer-reviewed journals and conferences. He also holds a U.S. patent. His research interests include the stochastic modeling and analysis of computer and communication systems, physical layer and MAC layer of vehicular ad hoc wireless networks, computational intelligence and its applications to coding, signal processing, and control, quality of service, and call admission control protocols in wireless networks. He is a Senior Member of the IEEE. He is (or was) a PI, a Co-PI, or a Project Leader in several projects sponsored by NSF, NSF EPSCoR, Motorola, Chinese NSF, AFOSR, and ARO. He was a recipient of the Best Paper Award at the IEEE International Conference on Network Infrastructure and Digital Content. He is a Guest Editor of the Special Issue on Reliable and secure VANETs in the IEEE TRANSACTIONS ON DEPENDABLE AND SECURE COMPUTING.

JIN WANG received the B.S. and M.S. degrees from the Nanjing University of Posts and Telecommunications, China, in 2002 and 2005, respectively, and the Ph.D. degree from Kyung Hee University, South Korea, in 2010. He is currently a Professor with the Changsha University of Science and Technology. He has published more than 300 international journal and conference papers. His research interests mainly include wireless sensor networks, network performance analysis, and optimization. He is a Senior Member of the IEEE and a member of ACM.

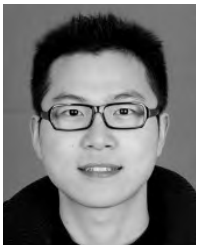

BAOFENG JI received the Ph.D. degree in information and communication engineering from Southeast University, Nanjing, China, in 2013, where he has been a Postdoctoral Fellow with the School of Information Science and Engineering, since 2015. He has also been an Assistant Professor with the Henan University of Science and Technology, since 2013. He has authored or co-authored more than 40 papers and holds several patents. His current research interests include signal processing for wireless communications, MIMO communications, cooperative relaying systems, and statistical signal processing.

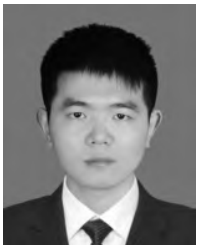

CHUNHAI FENG received the B.S. and M.S. degrees from Soochow University, China, in 2012 and 2015, respectively. He is currently pursuing the Ph.D. degree in computer engineering with The University of Texas at Arlington. His research interests include wireless communications, computer networks, and machine learning.

JINXIU SI received the B.S. degree from the Department of Electronic Information Engineering, Huaihai Institute of Technology, Lianyungang, China, in 2015. He is currently pursuing the M.S. degree with the School of Information and Telecommunication Engineering, University of Electronic Science and Technology of China, Chengdu, China. His current research interests include radar target recognition, pattern recognition, and deep learning.